



OPEN

Unlocking the human inner ear for therapeutic intervention

Hao Li¹, Sumit Agrawal^{2,3,4,5}, Seyed Alireza Rohani², Ning Zhu^{6,7}, Daniela I. Cacciabue⁸, Marcelo N. Rivolta^{8,14}, Douglas E. H. Hartley^{9,10,11,14}, Dan Jiang^{12,13,14}, Hanif M. Ladak^{2,3,4,5,14,15}, Gerard M. O'Donoghue^{9,10,14,15} & Helge Rask-Andersen^{1,14,15}✉

The human inner ear contains minute three-dimensional neurosensory structures that are deeply embedded within the skull base, rendering them relatively inaccessible to regenerative therapies for hearing loss. Here we provide a detailed characterisation of the functional architecture of the space that hosts the cell bodies of the auditory nerve to make them safely accessible for the first time for therapeutic intervention. We used synchrotron phase-contrast imaging which offers the required microscopic soft-tissue contrast definition while simultaneously displaying precise bony anatomic detail. Using volume-rendering software we constructed highly accurate 3-dimensional representations of the inner ear. The cell bodies are arranged in a bony helical canal that spirals from the base of the cochlea to its apex; the canal volume is 1.6 μL but with a diffusion potential of 15 μL . Modelling data from 10 temporal bones enabled definition of a safe trajectory for therapeutic access while preserving the cochlea's internal architecture. We validated the approach through surgical simulation, anatomical dissection and micro-radiographic analysis. These findings will facilitate future clinical trials of novel therapeutic interventions to restore hearing.

By 2050, disabling hearing loss due to damage to the sensorineural structures of the inner ear will affect over 700 million individuals globally with major health, economic and societal implications¹. Yet no biological treatment exists for this disabling condition. Auditory prostheses, such as hearing aids and cochlear implants, represent the mainstay of current management but have considerable functional limitations. The greatest challenge to-day is to find a curative treatment for hearing loss through restoration of the neurosensory substrates that underpin our ability to hear. This challenge is formidable as the human cochlea is a highly specialised post-mitotic organ with highly restricted proliferative and regenerative capabilities. The cochlea's sensory receptors comprise vibration-sensitive hair cells, their synapses and the neurones that subservise them. The system is exquisitely finetuned and can respond within millionths of a second to displacement of atomic dimensions. These neurosensory structures are fragile and may be permanently lost due to genetic and environmental factors and are particularly susceptible to the ageing process. The hearing loss may be due to a loss of hair cells², synaptic dysfunction³ or to depletion of the neural population within the cochlea⁴ as well as a dysfunction of the stria vascularis and fibrocyte network⁵. The alarming rise in prevalence of hearing loss, now affecting 7% of the world's population, is a major stimulus to exploit the potential of regenerative medicine in this field⁶.

Hampering progress has been the inaccessibility of the human cochlea which lies in the skull base deeply encased in the hardest bone in the human body. Yet, once accessed, the cochlea promises to be a receptive organ for neurosensory regeneration: the neurosensory cells are relatively few in number and its minute fluid

¹Department of Surgical Sciences, Otorhinolaryngology and Head and Neck Surgery, Uppsala University, Uppsala, Sweden. ²Department of Otolaryngology-Head and Neck Surgery, Western University, London, ON, Canada. ³Department of Medical Biophysics, Western University, London, ON, Canada. ⁴Department of Electrical and Computer Engineering, Western University, London, ON, Canada. ⁵School of Biomedical Engineering, Western University, London, ON, Canada. ⁶Canadian Light Source, Saskatoon, Canada. ⁷Department of Chemical and Biological Engineering, College of Engineering, University of Saskatchewan, Saskatoon, Canada. ⁸School of Biosciences, Centre for Stem Cell Biology, University of Sheffield, Sheffield, UK. ⁹National Institute for Health Research (NIHR) Nottingham Biomedical Research Centre, Nottingham, UK. ¹⁰Queens Medical Centre, Nottingham University Hospitals NHS Trust, Nottingham, UK. ¹¹Otology and Hearing Group, Division of Clinical Neuroscience, School of Medicine, University of Nottingham, Nottingham, UK. ¹²Centre for Craniofacial and Regenerative Biology, King's College London, London, UK. ¹³Hearing Implant Centre, Guy's and St. Thomas' NHS Foundation Trust, London, UK. ¹⁴These authors contributed equally: Marcelo N. Rivolta, Douglas E. H. Hartley, Dan Jiang, Hanif M. Ladak, Gerard M. O'Donoghue and Helge Rask-Andersen. ¹⁵These authors jointly supervised this work: Hanif M. Ladak, Gerard M. O'Donoghue and Helge Rask-Andersen. ✉email: dan.jiang@kcl.ac.uk; Helge.Rask-Andersen@surgsci.uu.se

compartments (with a total volume around 200 μL) are tightly confined with a negligible circulation which should facilitate biological effectiveness and restricted biodistribution, minimising off-target effects. In addition, cochlear tissues are relatively immune-privileged being protected by the blood-labyrinth barrier thus dampening the inflammatory rejection process. Recent elaboration of a range of molecular mechanisms responsible for inner ear dysfunction have opened a vista of opportunities for a range of novel therapeutic approaches to hearing loss including small molecules, gene and cell therapies⁷. Central to success, however, is the ability to deliver these agents safely and precisely to their target structures within the relatively impenetrable human cochlea. Encouraging evidence from non-human mammalian studies have shown that targeted administration of human stem cell-derived otic progenitors can result in hearing restoration⁸. To exert their therapeutic effects, otic progenitors were delivered precisely to their target structures in the cochlear neural space of gerbils (Supplementary Fig. 1). Until now, an equivalent access has not been available for the human cochlea. In this report we focus on the human spiral ganglion (HSG) cell population, aiming to create for the first time an accurate three-dimensional model, analysing its detailed functional cytoarchitecture and how it might be safely accessed for regenerative interventions in humans.

The structures of the cochlea, such as the basilar and Reissner's membranes, are microscopic and well beyond the resolution of clinical imaging modalities. Although micro-computed tomography provides sufficient spatial resolution, contrast agents are necessary to discern soft tissues but may lead to tissue shrinkage⁹. Conventional histological techniques, have been susceptible to dissection, decalcification and staining artefacts. We thus used synchrotron radiation phase-contrast imaging (SR-PCI) to delineate these minute structures while leaving them in situ. Several synchrotron studies applied to the inner ear have been published recently^{10–12}, but here we have greatly extended this work to define and validate a novel therapeutic corridor to the human inner ear. SR-PCI differs from conventional radiography in being able to allow a phase shifted beam to interact with the original beam to produce fringes that represent the structural and surface boundaries (edge enhancement) of a specimen. This phase-contrast imaging produces images with excellent soft-tissue and bone discrimination and made it possible to accurately image the detailed cytoarchitecture of the human inner ear, in particular to access the structures that harbour the cochlear neurons in the intact state without incurring artefacts that so compromised previous anatomical studies. The use of advanced computer vision tools enabled fine blood vessels to be imaged and the pathways of nerves to be tracked through to the bony core (or modiolus) of the cochlea. This level of detail subsequently informed the planning of a safe surgical approach for clinical application.

Results

Rosenthal's canal (RC), which houses the cell bodies of the 30 to 35,000 human spiral ganglion (HSG) neurons of the auditory nerve, hugs the modiolus and extends from its base to near the cochlear apex (Fig. 1). The physical characteristics of RC are described in Table 1 (and Supplementary Table 1). Our analysis determined that it averages 14.57 mm in length (range 14.02–15.08 mm) and that it is covered by bone with a thickness of 28–56 μm which may be deficient in parts. The diameter of RC varies from 0.1 to 0.5 mm, being at its greatest towards the apex of the helix and has an average volume of 1.6 mm³ (Supplementary Fig. 2). The central projections of the auditory nerve traverse a virtual space containing cerebrospinal fluid as they exit the cochlea on their way to the brain-stem (Supplementary Fig. 3). We calculated this space to have a potential volume of 15 mm³ and as these nerve fibres are devoid of perineurium and may thus be receptive to cell or gene-based therapies.

Fortunately, at the base of the cochlea the RC lies in close proximity to the round window membrane (Fig. 1 and Supplementary Fig. 4), a structure that is easily identifiable during routine ear surgery and that can be readily penetrated or reflected to gain access to RC. We thus used our SR-PCI 3-dimensional models to define the round window to RC relationships and then undertook a series of surgical simulations, formulating a heat map to define the surgical trajectory that would lead directly to RC with the highest probability (Fig. 2). We found that by using a dynamic grid adjusted to the size of the round window that setting the point of penetration superiorly would reach target in 80% of cases without compromising cochlear blood supply which runs immediately adjacent (Supplementary Fig. 5 and Supplementary Table 2). Depending on the trajectory used, the contents of RC lay just 3–4 mm deep to the round window. Furthermore, to facilitate clinical translation, we ensured the trajectories we planned were consistent with instrumentation and approaches compatible with those used in routine ear surgery (Supplementary video).

In order to confirm the validity of our proposed access, we carried out a series of anatomical micro-dissections on human temporal bones. The aim was to determine if RC could be reached using surgical approaches through the mastoid bone with standard instrumentation. Six temporal bones were used, with surgeons marking the expected site of RC by positioning a radio-opaque metallic marker. The specimens were scanned prior to dissection (to exclude structural anomalies) as well as following placement of the marker. The bones were scanned with micro-computed tomography, following a protocol described elsewhere¹³. In 5 of the 6 temporal bones, the marker was either within the RC or immediately adjacent to it results that were in line with those predicted from our modelling data; in one bone the marker ended up fractionally below target (Supplementary Fig. 6). In none of the temporal bones was the microvasculature disrupted and no unintended damage to other anatomical structures within the ear was observed.

Discussion

The inability to adequately image the fine structures of the human inner ear has been a major barrier to advance therapies for this complex end-organ. SR-PCI is proving to be transformative in displaying and evaluating these microscopic structures providing unprecedented visualisation of its in-situ cytoarchitecture. Traditional methods used to design surgical routes to the cochlea, even with operating microscopes, were marred by their inherent destructive nature. We have demonstrated, that 3-dimensional models based on SR-PCI data allow the

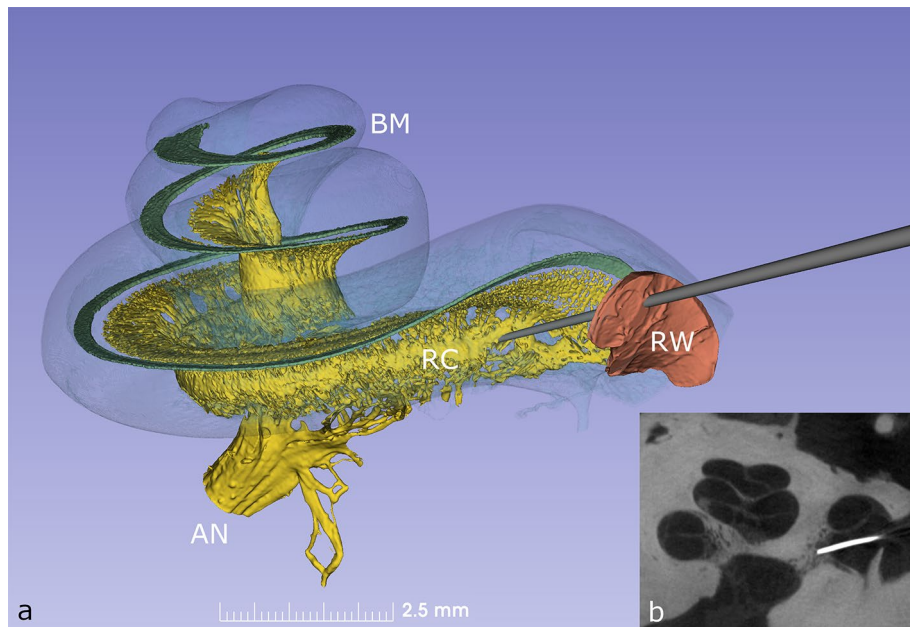


Figure 1. (a) Synchrotron phase contrast imaging (SR-PCI) with 3D orthographic rendering of an intact left human inner ear. The bony wall of the cochlea was made semi-transparent to permit visualization of the basilar membrane (BM), Rosenthal's canal (RC) and auditory nerve (AN). The auditory nerve contains approx. 30,000 fibres and their cell bodies are located in a 14.5 mm long spiral bony canal called RC. From there, peripheral neurites spread out to innervate approx. 15,000 hair cells placed on the BM. A probe is shown penetrating the round window (RW) membrane to access the underlying RC. (b) Microradiograph taken following placement of a radio-opaque marker at the presumed site of RC on anatomical dissection; the image confirms precise targeting of RC during dissection.

Bone #	RC length (mm)	RC diameter (mm)			RC volume (mm ³)
	Total	RC base	45°	90°	Total
1	14.02	0.133	0.291	0.435	1.182
2	14.73	0.100	0.366	0.498	1.376
3	14.28	0.109	0.395	0.464	1.087
4	14.61	0.060	0.442	0.430	1.392
5	14.22	0.116	0.432	0.495	1.668
6	15.08	0.143	0.382	0.464	1.746
7	14.91	0.103	0.482	0.590	1.246
8	14.58	0.109	0.494	0.567	2.315
9	14.27	0.122	0.468	0.444	2.012
10	14.98	0.096	0.519	0.637	2.150
Average	14.568	0.109	0.427	0.502	1.617
SD	0.36058	0.023	0.069	0.072	0.430

Table 1. The length, diameter and volume of Rosenthal's Canal (RC) as determined by synchrotron phase-contrast imaging in the 10 human temporal bones in the study. The diameter of the RC is larger with increasing distance from the base of the cochlea.

conception of highly accurate intervention pathways which were subsequently validated by anatomical dissection and micro-radiographic imaging. These findings will greatly facilitate the accurate delivery of novel therapeutic agents to their target structures in the inner ear and will thus derisk future clinical trials. The application of SR-PCI to the auditory system also dovetails with an escalation of interest in regenerative inner ear therapies which hold considerable promise for addressing the growing health burden of hearing loss^{14–16}. While considerable challenges remain in developing novel therapeutics for use in humans¹⁷, we believe that these developments herald a new era for the application of regenerative therapeutics to the inner ear. Although SR-PCI cannot be used in humans *in vivo* its translational value is immense through enabling precise modelling of the inner ear microstructures to guide therapeutic access. These models can be further enhanced by automatic segmentation and deep-learning networks to improve accuracy and support clinical application²².

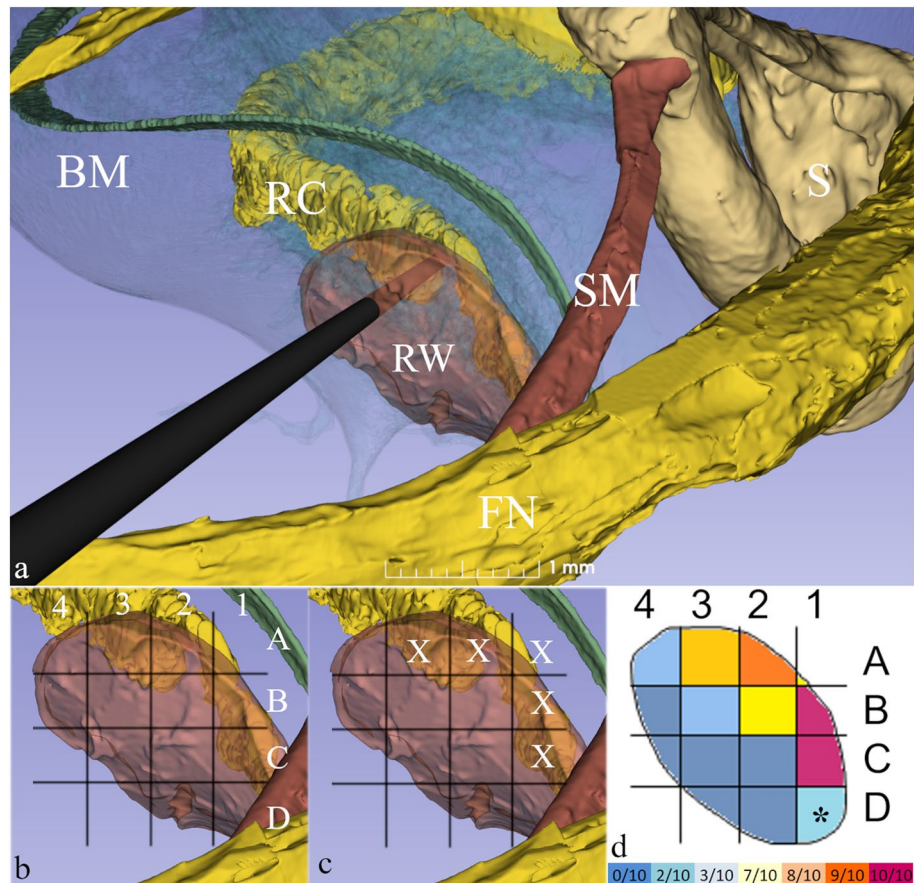


Figure 2. (a) The surgical approach to left Rosenthal's Canal (RC) passing through the mastoid bone behind the ear. Note the structures of surgical interest: the facial nerve (FN), the stapes (S) and stapedius muscle (SM) and round window membrane (RW). A surgical trephine is seen penetrating the RW to reach RC located just deep to it. (b) A 4 × 4 dynamic grid was applied to 10 RW membranes and was adjusted to membrane size for each specimen. (c) X denotes those grid units in closest anatomical proximity to RC in which a given penetration had at least an 80% chance of reaching RC (see Supplementary Table 2). (d) Using this data, a heat map was created for optimal targeting of RC behind the RW membrane. Highest probability of targeting the RC was through the superior mid-region of the RW membrane. At A2 and A3, the chance was 90% and 80% respectively. Higher values were noted in C1 and B1 (100%), but this region risks injury to the vestibulo-cochlear artery. *D1 was covered by stapedius muscle and was thus not evaluable. Colour bar at the bottom displays the actual frequencies of successfully targeting the RC.

Material and methods

Ten adult human temporal bones were obtained with permission from the Body Bequeathal Program at Western University, London, Ontario, Canada in accordance with and approved by the Anatomy Act of Ontario and Western University's Committee for Cadaveric Use in Research (approval #19062014). The imaging technique used in this study is the propagation-based X-ray phase-contrast imaging (PCI) method, which is also known as in-line PC and has previously been adopted by us to image the auditory system^{18–20}. Compared to conventional X-ray absorption based imaging, in-line PCI uses X-ray refraction which highlights tissue boundaries within a sample. It can be used to image soft tissues which do not absorb X-rays sufficiently to distinguish tissue components based on image contrast. A spatially coherent source is needed for in-line PCI, hence synchrotron radiation is used in this work rather than a conventional X-ray source. The overall set-up for in-line PCI is similar to typical absorption based radiography in that it consists of a source, a sample, and a detector; however, the main difference is that the detector is placed further from the sample when using in-line PCI, and this gives rise to Fresnel fringes. In-line PCI is sensitive to changes in refractive index which leads to edge enhancement in images.

SR-PCI scanning was performed at the Bio-Medical Imaging and Therapy (BMIT) 05ID-2 beamline at the Canadian Light Source Inc. located in Saskatoon, SK, Canada. The X-ray photon energy was 42 keV, with sample-to-source distance of 57 m and sample-to-detector distance of 2 m. The detector had field of view of 36 mm × 9.5 mm and pixel size of 9 μm, and 3000 projections were collected over 180° rotation. The reconstruction was performed using the UFO platform (www.github.com/ufo-kit), which is an open-source platform. To perform the quantitative analysis and 3D visualization, phase-retrieval technique was used to convert the edge enhancement caused by fringes, to areal contrast using Paganin/TIE method²¹. The reconstructed slices were then imported to 3D Slicer (www.slicer.org) for visualization, segmentation and measurements^{18–20}. Manual threshold

painting was performed for most anatomical structures. Measurements of volumes and distances to adjacent critical structures was then undertaken and trajectory maps for future surgical approaches were designed. Image segmentation was driven by the need to survey the anatomical structures of clinical interest. Semi-automatic and manual segmentation tools, threshold painting, thresholding, tractography, and scissors tools were used to display the fine detail of the structures of interest.

Ethics approval. Permission was obtained from the Body Bequeathal Program at Western University, London, Ontario, Canada in accordance with and approved by the Anatomy Act of Ontario and Western University's Committee for Cadaveric Use in Research (approval #19062014).

Data availability

All data generated or analysed during this study are included in this published article and its supplementary information files.

Received: 15 June 2022; Accepted: 11 October 2022

Published online: 08 November 2022

References

1. WHO World Report on Hearing 2021 (2021). (3/3/2021), <https://www.who.int/publications/i/item/world-report-on-hearing> Global report ISBN: 9789240020481
2. Hudspeth, A. J. Integrating the active process of hair cells with cochlear function. *Nat. Rev. Neurosci.* **15**, 600–614 (2014).
3. Liberman, M. C. & Kujawa, S. G. Cochlear synaptopathy in acquired sensorineural hearing loss: Manifestations and mechanisms. *Hear. Res.* **349**, 138–147 (2017).
4. Zhang, T., Dorman, M. F., Gifford, R. & Moore, B. C. J. Cochlear dead regions constrain the benefit of combining acoustic stimulation with electric stimulation. *Ear Hear.* **35**, 410–417 (2014).
5. Furness, D. N. Forgotten fibrocytes: A neglected, supporting cell type of the cochlea with the potential to be an alternative therapeutic target in hearing loss. *Front. Cell. Neurosci.* **2019**, 13 (2019).
6. Wilson, B. S., Tucci, D. L., Merson, M. H. & O'Donoghue, G. M. Global hearing health care: New findings and perspectives. *Lancet (Lond., Engl.)* **390**, 2503–2515 (2017).
7. Korver, A. M. H. *et al.* Congenital hearing loss. *Nat. Rev. Dis. Prim.* **3**, 1 (2017).
8. Chen, W. *et al.* Restoration of auditory evoked responses by human ES-cell-derived otic progenitors. *Nature* **490**, 278–282 (2012).
9. Buytaert, J., Goyens, J., De Greef, D., Aerts, P. & Dirckx, J. Volume shrinkage of bone, brain and muscle tissue in sample preparation for micro-CT and light sheet fluorescence microscopy (LSFM). *Microsc. Microanal.* **20**, 1208–1217 (2014).
10. Schart-Morén, N., Agrawal, S. K., Ladak, H. M., Li, H. & Rask-Andersen, H. Effects of various trajectories on tissue preservation in cochlear implant surgery: A micro-computed tomography and synchrotron radiation phase-contrast imaging study. *Ear Hear.* **40**, 393–400 (2019).
11. Li, H. *et al.* Vestibular organ and cochlear implantation—a synchrotron and micro-CT study. *Front. Neurol.* **12**, 5 (2021).
12. Lareida, A. *et al.* High-resolution X-ray tomography of the human inner ear: Synchrotron radiation-based study of nerve fibre bundles, membranes and ganglion cells. *J. Microsc.* **234**, 95–102 (2009).
13. Schart-Morén, N., Larsson, S., Rask-Andersen, H. & Li, H. Three-dimensional analysis of the fundus of the human internal acoustic canal. *Ear Hear.* **39**, 563–572 (2018).
14. Andres-Mateos, E. *et al.* Choice of vector and surgical approach enables efficient cochlear gene transfer in nonhuman primate. *Nat. Commun.* **13**, 1359 (2022).
15. Lustig, L. & Akil, O. Cochlear gene therapy. *Cold Spring Harb. Perspect. Med.* **9**, 3191 (2019).
16. Crane, R., Conley, S. M., Al-Ubaidi, M. R. & Naash, M. I. Gene therapy to the retina and the cochlea. *Front. Neurosci.* <https://doi.org/10.3389/fnins.2021.652215> (2021).
17. Plontke, S. K. & Salt, A. N. Local drug delivery to the inner ear: Principles, practice, and future challenges. *Hear. Res.* **368**, 1–2 (2018).
18. Elfarawany, M. *et al.* Micro-CT versus synchrotron radiation phase contrast imaging of human cochlea. *J. Microsc.* **265**, 349–357 (2017).
19. Koch, R. W., Ladak, H. M., Elfarawany, M. & Agrawal, S. K. Measuring Cochlear Duct Length—a historical analysis of methods and results. *J. Otolaryngol. Head Neck Surg.* **46**, 19 (2017).
20. Mei, X. *et al.* Vascular supply of the human spiral ganglion: Novel three-dimensional analysis using synchrotron phase-contrast imaging and histology. *Sci. Rep.* <https://doi.org/10.1038/s41598-020-62653-0> (2020).
21. Paganin, D., Mayo, S. C., Gureyev, T. E., Miller, P. R. & Wilkins, S. W. Simultaneous phase and amplitude extraction from a single defocused image of a homogeneous object. *J. Microsc.* **206**, 33–40 (2002).
22. Nikan, S. *et al.* PWD-3DNet: A deep learning-based fully-automated segmentation of multiple structures on temporal bone CT scans. *IEEE Trans. Image Process.* **30**, 739–753 (2021).

Acknowledgements

The research was funded by a grant from Rinri Therapeutics administered by the University of Nottingham. Part of the research was funded by Swedish Hearing Research Foundation. Part of the research described in this paper was performed at the Canadian Light Source, a national research facility of the University of Saskatchewan, which is supported by the Canada Foundation for Innovation (CFI), the Natural Sciences and Engineering Research Council (NSERC), the National Research Council (NRC), the Canadian Institutes of Health Research (CIHR), the Government of Saskatchewan, and the University of Saskatchewan. We are grateful to Matthew B. Farr for the 3D reconstruction that helped with the preparation of Supplementary Fig. 1 and to Faizah Mushtaq for project administration.

Author contributions

Author contributions: Conceptualization: all authors contributed equally Synchrotron imaging: S.A.R., N.Z., S.A., H.M.L. Modelling and Validation: H.L., D.E.H., D.J., G.M.O'D, H.R.A. Writing—original draft: G.M.O'D; Writing-review & editing: all authors contributed equally.

Funding

Open access funding provided by Uppsala University.

Competing interests

Marcelo N. Rivolta is the Founder and Chief Scientific Officer of Rinri Therapeutics. All other authors have no competing/conflict of interest.

Additional information

Supplementary Information The online version contains supplementary material available at <https://doi.org/10.1038/s41598-022-22203-2>.

Correspondence and requests for materials should be addressed to D.J. or H.R.-A.

Reprints and permissions information is available at www.nature.com/reprints.

Publisher's note Springer Nature remains neutral with regard to jurisdictional claims in published maps and institutional affiliations.



Open Access This article is licensed under a Creative Commons Attribution 4.0 International License, which permits use, sharing, adaptation, distribution and reproduction in any medium or format, as long as you give appropriate credit to the original author(s) and the source, provide a link to the Creative Commons licence, and indicate if changes were made. The images or other third party material in this article are included in the article's Creative Commons licence, unless indicated otherwise in a credit line to the material. If material is not included in the article's Creative Commons licence and your intended use is not permitted by statutory regulation or exceeds the permitted use, you will need to obtain permission directly from the copyright holder. To view a copy of this licence, visit <http://creativecommons.org/licenses/by/4.0/>.

© The Author(s) 2022